Available online at www.ijpsdr.com

International Journal of Pharmaceutical Sciences and Drug Research
2018; 10(4): 217-226

Research Article

ISSN: 0975-248X
CODEN (USA): IJPSPP

In silico Validation of Anti-Russell's Viper Venom Activity in *Phyllanthus emblica* L. and *Tamarindus indica* L.

V Deepa, S Sreekumar*, CK Biju

Biotechnology and Bioinformatics Division, Saraswathy Thangavelu Centre, KSCSTE-Jawaharlal Nehru Tropical Botanic Garden and Research Institute, Puthenthope, Thiruvananthapuram-695 586, Kerala, India

ABSTRACT

To validate the efficacy of viper anti-venom activity, a total of 79 phytochemicals from *Phyllanthus emblica* and 59 phytochemicals from *Tamarindus indica* were docked against each of the nine selected viper venom proteins such as basic phospholipase A2 VRV-PL-VIIIa, anticoagulant class II phospholipase A2, acidic phospholipase A2 Drk-a1, neutral phospholipase A2 RVV-PFIIc, L-amino acid oxidase, Russell's viper venom serine proteinase, RVV-V, cytotoxin drCT-1, dabocetin alpha subunit and cysteine-rich secretory protein Dr-CRPK using the tool Autodock. The structure of three proteins *viz* basic phospholipase A2 VRV-PL-VIIIa (PDB id-1OXL), anticoagulant class II phospholipase A2 (PDB id- 1VIP) and Russell's viper venom serine proteinase RVV-V (PDB id- 3S9A) were downloaded from RCSB Protein Data Bank and remaining targets 3D structures except neutral phospholipase A2 RVV-PFIIc were modelled using the tool SWISS-MODEL. The templates for modelling the structures were selected through BLASTp analysis. The structure of the neutral PLA2 was modelled using the tool I-TASSER. The stability of all the modelled structures were confirmed by Ramachandran Plot and the active site were detected using the tool MetaPocket2. The docked results revealed that both plants contain several inhibitory molecules against all the target proteins and certain compounds such as stigmasterol, β-sitosterol and campesterol, were present in both plants and each of these molecule can inhibit all venom proteins. The overall results substantiate the traditional use of these plants as antidote to snake bites. However, *in vitro* and *in vivo* experimental demonstration is essential for practical application of forgoing findings.

Keywords: Russell's viper, Docking, *In silico* screening, *Phyllanthus emblica, Tamarindus indica*.

DOI: 10.25004/IJPSDR.2018.100403 **Int. J. Pharm. Sci. Drug Res. 2018; 10(4): 217-226**

***Corresponding author**: Dr. S Sreekumar
Address: Biotechnology and Bioinformatics Division, Saraswathy Thangavelu Centre, KSCSTE-Jawaharlal Nehru Tropical Botanic Garden and Research Institute, Puthenthope, Thiruvananthapuram-695 586, Kerala, India
Tel.: +91- 9446480968
E-mail ✉: drsreekumar@rediffmail.com
Relevant conflicts of interest/financial disclosures: The authors declare that the research was conducted in the absence of any commercial or financial relationships that could be construed as a potential conflict of interest.
Received: 02 May, 2018; **Revised:** 24 May, 2018; **Accepted**: 30 May, 2018; **Published:** 20 July, 2018

INTRODUCTION

Snakebite is an acute life threatening medical emergency particularly in tropical and subtropical countries where people are engaged in field oriented agricultural works. The high snakebite mortality rate in rural areas is mainly due to the lack of proper medical facility. Majority of the victims depend on traditional healers and such details are not documented properly. Therefore, the actual snakebite burden still remains as unclear. However, based on available data it was estimated that the annual death rate due to snakebite is ranging from 81,000 to 138,000 globally and in India 50,000 per annum. [1-2] It is not a pathogenic disease but considering the high death rate, the World Health Organization (WHO) had included it along with neglected tropical diseases. Among the venomous snake species in India Russell's viper (*Daboia russellii*) causes high rate of morbidity and mortality in South India. [3] Their envenomation induces local pain and tissue damage, characterised by swelling, blistering, bleeding, and necrosis at the bite site, sometimes extending to the whole limb. [4] It can also induces coagulopathy and platelet dysfunction, leading to spontaneous systemic haemorrhages and persistent bleeding from fang marks, wounds, or gums. Intracranial bleeding, including anterior pituitary haemorrhage, and multi-organ failure are common causes of death. [5] Snake venom is a complex mixture of toxic and non- toxic proteins that act synergistically to cause death of the prey and diverse biological activities. It constitutes phospholipase A2 (PLA2s), myotoxins, hemorrhagic metalloproteinases and other proteolytic enzymes, coagulant components, cardiotoxins, cytotoxins and neurotoxins. The venom components and its functions are well described. [6-7]

The antivenom serum therapy is the only available treatment in modern medicine but its administration has several limitations such as anaphylaxis, pyrogen reaction and serum sickness, and variation in venom composition, identification of snake species and non-availability of storage facility in rural areas, high cost, etc. are the major obstacles in anti-venom therapy. [8] In fact, majority of the snakebite victims depend on herbal medicines which contain a plethora of phytomolecules having activity on biological molecules. The innumerable number of phytomolecules in herbal medicine may interacts each other and form a balanced state which can act individually, synergistically and cumulatively on biological molecules like proteins, peptides and rectify its abnormal functioning or enhance its activity. Demonstration of the mechanism of such activity through *in silico* method and subsequent confirmation in biological system through *in vitro* and *in vivo* experiments can give scientific evidence to the use of herbal medicine and its global acceptance. Since time immemorial *Phyllanthus emblica* L. and *Tamarindus indica* L. have been used against viper envenomation. [9-10] In the present investigation, the foregoing activity of these plants has been validated through *in silico* method and identified potential lead molecules.

MATERIALS AND METHODS

Preparation of Russell's viper venom proteins

Nine Russell's viper venom proteins which are already reported in the venom of Indian Russell's viper (*Daboia russelii*) viz. basic phospholipase A2 VRV-PL-VIIIa, anticoagulant class II phospholipase A2, acidic phospholipase A2 Drk-a1, neutral phospholipase A2 RVV-PFIIc, L-amino acid oxidase, Russell's viper venom serine proteinase RVV-V, cytotoxin drCT-1, dabocetin alpha subunit and cysteine-rich secretory protein Dr-CRPK were selected as the target molecules. The 3D structures of the target proteins viz. basic phospholipase A2 VRV-PL-VIIIa (PDB id-1OXL), anticoagulant class II phospholipase A2 (PDB id- 1VIP) and Russell's viper venom serine proteinase RVV-V (PDB id- 3S9A) were downloaded from RCSB Protein Data Bank. Water molecules and natural ligands present in these proteins were removed using SwissPdbViewer and prepared for docking. The 3D structures of acidic phospholipase A2 Drk-a1, L-amino acid oxidase, cytotoxin drCT-1, dabocetin alpha subunit and cysteine-rich secretory protein Dr-CRPK were modelled using the tools SWISS-MODEL and the structure of neutral phospholipase A2 RVV-PFIIc was modelled using the tool I-TASSER. To model the 3D structures, the primary amino acid sequences were retrieved from NCBI web site. They are acidic phospholipase A2 Drk-a1 (UniProtKB/Swiss-Prot ID-A8CG86.1), L-amino acid oxidase (UniProtKB/Swiss-Prot ID - G8XQX1.1), cytotoxin drCT-1 (UniProtKB/Swiss-ProtID - P0C5H4.1), dabocetin alpha subunit (GenBank ADK22821.1), cysteine-rich secretory protein Dr-CRPK (GenBank: ACE73567.1) and neutral phospholipase A2 RVV-PFIIc (UniProtKB/Swiss-Prot: P0DKX1.1). Except neutral phospholipase A2 RVV-PFIIc, the 3D structures of others were modelled using the tools SWISS-MODEL and the structure of neutral phospholipase A2 RVV-PFIIc was modelled using the tool I-TASSER. As reported earlier [11] FASTA format of the selected primary sequence of each protein was retrieved, BLASTp was carried out and selected the template sequence based on the E-value or total query cover percentage. Then the multiple alignment file (.aln) generated using the template sequence on NCBI was uploaded into the swiss-model workspace for generating the protein 3D model. In order to evaluate the stability of the model, energy minimization was carried out by GROMOS96 force field and quality of the modelled structure was assessed by QMEAN scoring function. Ramachandran plot analysis of the modelled proteins was also carried out using PDBsum [12] (Fig. 1).

To generate the 3D structure of neutral phospholipase A2 RVV-PFIIc as followed by the procedure [13] the primary sequence (UniProtKB/Swiss-Prot: P0DKX1.1) in FASTA format was uploaded on the I-TASSER

online server. The server generated an output result containing predicted secondary structure, predicted solvent accessibility, predicted normalised B-factor, top ten threading templates used by I-TASSER and finally top 5 models predicted by I-TASSER. From the result best model was selected and Ramachandran plot analysis was done (Fig. 1). The active site residues of each target protein were identified using the tool MetaPocket2.

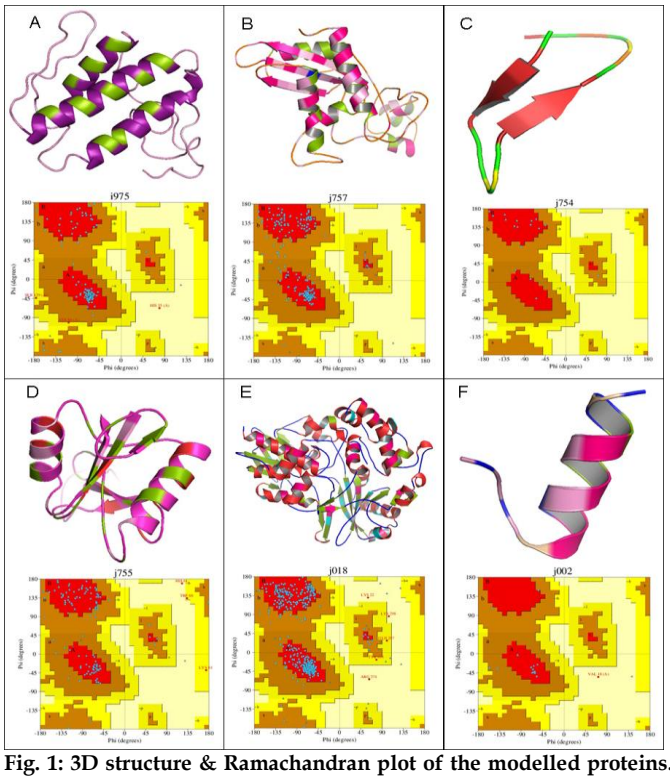

Fig. 1: 3D structure & Ramachandran plot of the modelled proteins. A- Acidic PLA2 Drk-a1, **B-** Cysteine-rich secretory protein Dr-CRPK, **C- Cytotoxin drCT-1, D-** Dabocetin alpha subunit, **E-L-amino acid oxidase, F-** neutral PL A2 RVV-PFIIc

Preparation of the ligand molecules

Based on traditional knowledge, literature and survey reports from traditional healers two plant species viz. *Phyllanthus emblica* L. and *Tamarindus indica* L. [9-10] were selected for the present study. A total number of 79 phytochemicals from *P. emblica* and 59 from *T. indica* were selected for screening and its 2D structures were collected from databases such as PubChem, Chemspider etc. The 3D structures of all phytochemicals in .pdb format were created using the tool CORINA (online tool for 3D structure creation). The list of phytochemicals used for the study is shown in Table 1.

Molecular Docking

Docking was performed between each of the nine selected target molecule and 114 selected ligand molecules using the tool AutoDock version 4.2 as reported earlier. [14] All docking parameters were kept as default. The numbers of grid points in xyz co-ordinates and spacing were set according to the size of each protein. The grid points assigned for docking to basic phospholipase A2 VRV-PL-VIIIa, anticoagulant class II phospholipase A2 and acidic phospholipase A2 Drk-a1 70×70×40, L-amino acid oxidase 70×50×50, Russell's viper venom serine proteinase, RVV-V 60×50×50, dabocetin alpha subunit 60×80×60, cysteine-rich secretory protein Dr-CRPK 60×60×60 and neutral phospholipase A2 RVV-PFIIc and cytotoxin drCT-1 40×40×40 respectively. The docked structures having free energy of binding <-5.0 kcal/mol were considered as active or hit molecules. Top five hit molecules were selected, analysed its binding stability based on hydrogen bond and other interactive forces and selected the best lead molecules.

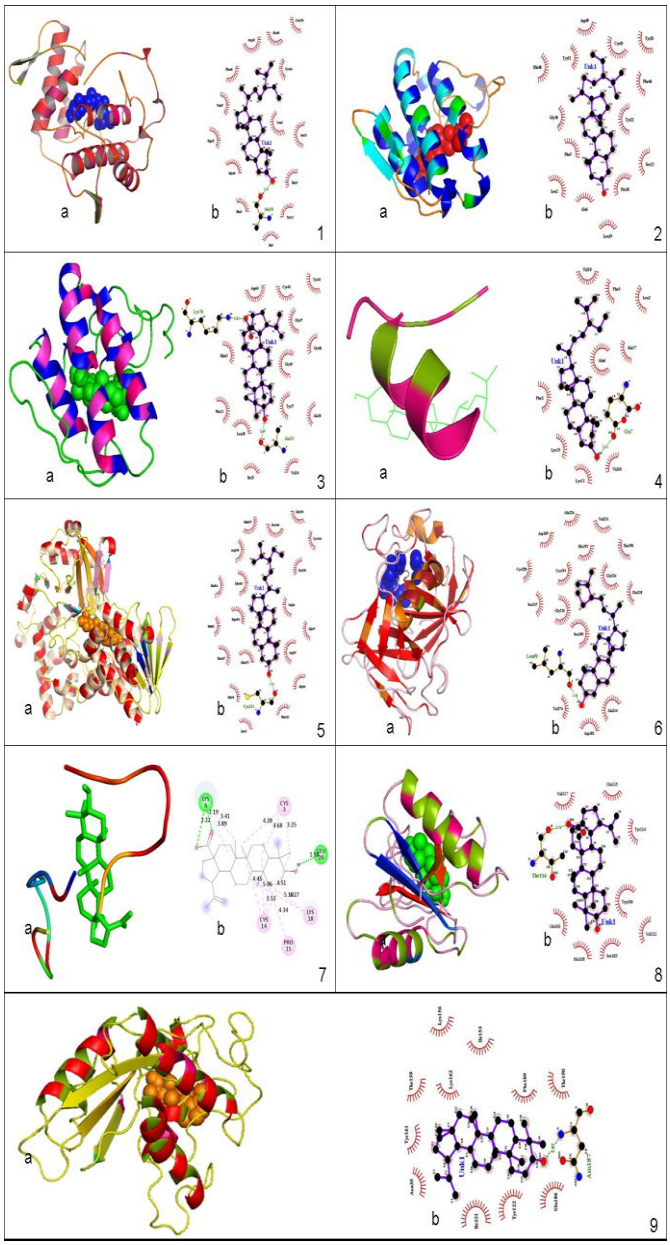

Fig. 2: Docked structures of Russell's viper venom proteins and lead molecules from *Phyllanthus. emblica* and interaction plot respectively: 1.(a & b) stigmasterol with basic PLA2 VRV-PL-VIIIa, **2.(a & b) β-sitosterol with** anticoagulant class II PLA2, **3.(a & b) betulinic acid with** acidic PLA2 Drk-a1, **4.(a & b) stigmasterol with** neutral PLA2 RVV-PFIIc, **5.(a & b) stigmasterol with L-amino acid oxidase, 6.(a & b) stigmasterol with** serine proteinase RVV-V, **7.(a & b) betulinic acid with cytotoxin drCT-1, 8.(a & b) betulonic acid with** dabocetin α-subunit, **9.(a & b) lupenone with cysteine-rich secretory protein** Dr-CRPK.

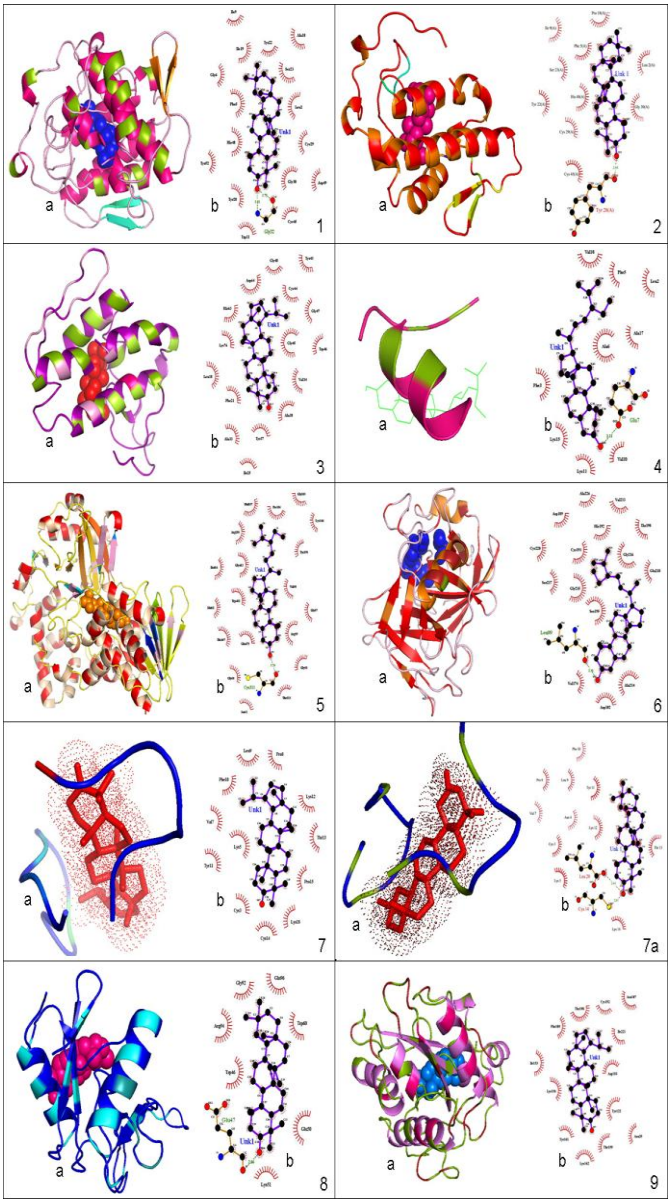

Fig. 3: Docked structures of Russell's viper venom proteins and lead molecules from *Tamarindus indica* and interaction plot respectively: 1.(a & b) β amyrin with basic PLA2 VRV-PL-VIIIa**, 2.(a & b) β amyrin with anticoagulant** class II PLA2**, 3.(a & b) lupanone with acidic PLA2 Drk-a1, 4.(a & b) stigmasterol with , neutral** PLA2 RVV-PFIIc**, 5.(a & b) stigmasterol with L-amino acid oxidase, 6.(a & b) stigmasterol with** serine proteinase RVV-V**, 7.(a & b) lupanone & 7a.(a & b)β amyrin with cytotoxin drCT-1, 8.(a & b) betulonic acid with** dabocetin α-subunit**, 9.(a & b) lupenone with cysteine-rich secretory protein** Dr-CRPK**.**

RESULT AND DISCUSSION

The Russell's viper venom consists of 90% proteins, of these up to 70% constitutes Phospholipase A2 (PLA2) which is present as at least seven isoforms [15] among the sub species of *Daboia russellii*. Four isoforms of PLA2 such as basic phospholipase A2 VRV-PL-VIIIa, anticoagulant class II phospholipase A2, acidic phospholipase A2 Drk-a1 and neutral phospholipase A2 RVV-PFIIc were used as targets in the present study. PLA2 damage mitochondria, red blood cells, leucocytes, platelets, peripheral nerve endings, skeletal muscle, vascular endothelium, and other membranes, producing presynaptic neurotoxic activity, cardiotoxicity, myotoxicity, necrosis, hypotension, haemolysis, anti-coagulation, haemorrhage, plasma leakage (oedemaformation) and autopharmacological release of histamine and other autacoids. [16]

Of the nine target proteins selected for screening, the structure of basic phospholipase A2 VRV-PL-VIIIa, anticoagulant class II phospholipase A2 and Russell's viper venom serine proteinase RVV-V were retrieved from PDB. The structural information of basic phospholipase A2 VRV-PL-VIIIa and serine proteinase isolated from Indian Russell's viper was not available, so the PDB structure isolated from *Daboia russellii pulchella* (basic PLA2 VRV-PL-VIIIa) and *Daboia russellii siamensis* (Russell's viper venom serine proteinase RVV-V) were used for the study. The MetaPocket generated ligand binding sites of basic PLA2 VRV-PL-VIIIa and anticoagulant class II PLA2 contains 82 and 28 amino acid residues. From these residues, the catalytic residue Asp49 was selected as active residue for docking. Similarly, serine proteinase has 46 amino acid residues in its ligand binding site. His57 was selected as critical residue because it is one of the active residues in the catalytic triad. [7] The protein stimulate blood clotting with formation of fibrin in the blood stream and paradoxically results in incoagulable blood, because most of the fibrin clot is broken down immediately by the body's own plasmin fibrinolytic system. Within 30 minutes of the bite, heavy bleeding starts. [17] Proteolytic enzymes are particularly involved in the pathogenesis of tissue necrosis, hemorrhage and bleeding disorders. [18]

All other target molecules structures except neutral PLA2 RVV-PFIIc were modelled using the tool SWISS-MODEL Expasy following homology modelling. The primary sequence (UniProtKB/Swiss-Prot: P0DKX1.1) used for modelling neutral PLA2 RVV-PFIIc constitute only 19 amino acid molecules and homology modelling in SWISS-MODEL needs minimum 30 amino acid molecules. Therefore, to model such a sequence I-TASSER server was used and modelling was done following thread modelling method.

Analysis of Modelled structures

A major protein content of Russell's viper venom is PLA2 which is present in the venom as isoenzymes. [15] On the basis of overall charge, the venom PLA2 isoenzymes were classified as acidic, basic and neutral. [19] The selected sequence of acidic PLA2 Drk-a1 has 138 amino acids and the BLASTp analysis indicated that acidic phospholipase A2 daboiatoxin A chain (PDB id-2H4C) showed 99% identity, 100% query cover and an E-value of 4e-97. Therefore, it was taken as the template for modelling the protein. Ramachandran plot analysis through PdbSum revealed that 91% of residues were present in most favoured region (Fig. 1). The MetaPocket generated ligand binding sites of acidic PLA2 Drk-a1contain 32 amino acid residues, from that Asp105 was selected as critical residue for docking. The primary sequence used for modelling neutral PLA2 RVV-PFIIc contains 19 amino acid molecules.

Table 1: List of phytochemicals from selected plants

Phyllanthus emblica

1. Stigmasterol ($C_{29}H_{48}O$)
2. Catechin ($C_{15}H_{14}O_6$)
3. Gallic acid ($C_7H_6O_5$)
4. β-sitosterol ($C_{29}H_{50}O$)
5. Hypophyllanthin ($C_{24}H_{30}O_7$)
6. Corilagin ($C_{27}H_{22}O_{18}$)
7. Methyl gallate ($C_8H_8O_5$)
8. Ascorbic acid ($C_6H_8O_6$)
9. (-)-epiafzelechin ($C_{15}H_{14}O_5$)
10. Chebulic acid ($C_{14}H_{15}O_{11}$)
11. Glucogallin ($C_{13}H_{17}O_{10}$)
12. Naringenin ($C_{15}H_{12}O_5$)
13. (+)-gallocatechin ($C_{15}H_{14}O_7$)
14. Chebulinic acid ($C_{41}H_{32}O_{27}$)
15. Phyllaemblicin C ($C_{38}H_{59}O_{23}$)
16. Phyllanemblinin A ($C_{27}H_{21}O_{17}$)
17. 1,6-di-o-galloyl-β-d-glucose ($C_{20}H_{21}O_{14}$)
18. Eriodictyol-7-O-glucoside ($C_{21}H_{22}O_{11}$)
19. Phyllaemblicin F ($C_{54}H_{79}O_{27}$)
20. Phyllanemblinin B ($C_{27}H_{23}O_{18}$)
21. β-amyrin-3-palmitate ($C_{46}H_{81}O_2$)
22. Phyllaemblicin D ($C_2H_{35}O_{13}$)
23. Phyllaemblicin A ($C_{27}H_{35}O_{14}$)
24. Phyllanemblinin C ($C_{41}H_{32}O_{26}$)
25. 5-hydroxymethylfurfural ($C_6H_6O_3$)
26. Phyllaemblicin E ($C_{38}H_{61}O_{23}$)
27. (-)-epicatechin ($C_{15}H_{14}O_6$)
28. Phyllanemblinin D ($C_{27}H_{29}O_{20}$)
29. 7,8,3′,4′-tetrahydroxyl-6-c-[α -l-rhamnopyranosyl-(1→2)]-b-d-glucopyranosyl flavone ($C_{21}H_{30}O_{11}$)
30. Luteolin-4'-neohesperidoside ($C_{27}H_{30}O_{15}$)
31. Kaempferol-3-rhamnoside ($C_{21}H_{20}O_{10}$)
32. Myricetin-3-O-rhamnoside ($C_{21}H_{20}O_{12}$)
33. Punicafolin ($C_{41}H_{30}O_{26}$)
34. Zeatin ($C_{10}H_{13}N_5O$)
35. Lupenone ($C_{30}H_{48}O$)
36. Pyrogallol ($C_6H_6O_3$)
37. Isostrictinnin ($C_{27}H_{23}O_{18}$)
38. Geranin A ($C_{30}H_{24}O_{10}$)
39. Amlaic acid ($C_{27}H_{24}O_{19}$)
40. Betulin ($C_{30}H_{50}O_2$)
41. Astragallin ($C_{21}H_{20}O_{11}$)
42. Ellagic acid ($C_{14}H_6O_8$)
43. Citric acid ($C_6H_8O_7$)
44. Progallin A ($C_9H_{10}O_5$)
45. 3-ethylgallicacid ($C_9H_{13}O_5$)
46. Emblicanin A ($C_{34}H_{22}O_{22}$)
47. Furosin ($C_{27}H_{23}O_{19}$)
48. Kaempferol ($C_{15}H_{10}O_5$)
49. β-amyrinketone ($C_{30}H_{48}O$)
50. Cinnamic acid ($C_9H_8O_2$)
51. Pedunculagin ($C_{34}H_{24}O_{22}$)
52. Eriodictyol ($C_{15}H_{12}O_5$)
53. Leucodelphinidin ($C_{15}H_{14}O_8$)
54. Epigallocatechin ($C_{15}H_{14}O_7$)
55. Phyllaemblic acid ($C_{21}H_{25}O_9$)
56. Putranjivain A (C47H52O31)
57. Chebulagic acid ($C_{41}H_{30}O_{27}$)
58. Campesterol ($C_{28}H_{48}O$)
59. Carpinusin ($C_{41}H_{30}O_{27}$)
60. Daucosterol ($C_{35}H_{60}O_5$)
61. Betulinic acid ($C_{30}H_{49}O_3$)
62. Lupeol ($C_{30}H_{50}O$)
63. β -humulene ($C_{15}H_{24}$)
64. Quercetin ($C_{15}H_{10}O_7$)
65. 1,2,6-trigalloylglucose ($C_{27}H_{24}O_{18}$)
66. Flavogallonic-acid-dilactone ($C_{21}H_{11}O_{12}$)
67. Neochebulagic-acid ($C_{41}H_{55}O_{28}$)
68. Dihydrokaempferol ($C_{15}H_{12}O_5$)
69. Betulonic acid ($C_{30}H_{47}O_3$)
70. Friedelan-3-one($C_{30}H_{50}O$)
71. Phyllantidin ($C_{13}H_{15}NO_3$)
72. Digallicacid ($C_{14}H_{10}O_9$)
73. Phyllanemblinin F ($C_{27}H_{29}O_{20}$)
74. Phyllanemblinin E ($C_{27}H_{29}O_{20}$)
75. Phyllaemblicin B ($C_{33}H_{45}O_{19}$)
76. Zeatin-riboside ($C_{15}H_{21}N_5O_5$)
77. Punigluconin ($C_{34}H_{27}O_{23}$)
78. Galactaric acid ($C_6H_{12}O_8$)
79. Emblicanin B ($C_{34}H_{20}O_{22}$)

Tamarindus indica

80. n-Nonadecanoate ($C_{19}H_{38}O_2$)
81. Cerotate (C26H51O2-)
82. Luteolin ($C_{15}H_{12}O_5$)
83. Naringenin ($C_{15}H_{12}O_5$)
84. 2,2'-diethoxy-5,5'-Bi-1-pyrroline ($C_{12}H_{20}N_2O_2$)
85. Methyl heptylate ($C_8H_{16}O_2$)
86. 1-malic acid ($C_4H_6O_5$)
87. 2-methylthiazole (C_4H_5NS)
88. 2,3-butanediol ($C_4H_{10}O_2$)
89. Cycloartanol ($C_{30}H_{52}O$)
90. Citric acid ($C_6H_{11}O_7$)
91. Palmitic acid ($C_{16}H_{32}O_2$)
92. 2-acetylfuran ($C_6H_6O_2$)
93. Epicatechin ($C_{15}H_{14}O_6$)
94. Geraniol ($C_{10}H_{18}O$)
95. Pinitol ($C_7H_{14}O_6$)
96. 2-ethylthiazole (C_5H_7NS)
97. Eriodictyol ($C_{15}H_{12}O_6$)
98. Orientin ($C_{21}H_{20}O_{11}$)
99. Oxalic acid ($C_2H_2O_4$)
100. Oleic acid ($C_{18}H_{34}O_2$)
101. Formic acid (CH_2O_2)
102. Lupanone ($C_{30}H_{50}O$)
103. Campesterol ($C_{28}H_{48}O$)
104. n-heptadecanoate ($C_{17}H_{33}O_2$-)
105. Nonanoic acid ($C_9H_{18}O_2$)
106. Pipecolic acid ($C_6H_{11}NO_2$)
107. Nonacosatrienoic acid ($C_{29}H_{52}O_2$)
108. β-sitosterol ($C_{29}H_{50}O$)
109. n-hexacosane ($C_{26}H_{54}$)
110. Vitexin ($C_{21}H_{20}O_{10}$)
111. Stigmasterol ($C_{29}H_{48}O$)
112. N-docosanoate ($C_{22}H_{44}O_2$)
113. Nicotinic acid ($C_6H_5NO_2$)
114. Lupeol ($C_{30}H_{50}O$)
115. 9-Decenoate ($C_{10}H_{17}O_2$-)
116. Acetic acid ($C_2H_4O_2$)
117. Isoorientin ($C_{21}H_{20}O_{11}$)
118. Tannin ($C_{27}H_{24}O_{18}$)
119. Tartaric acid ($C_4H_6O_6$)
120. Trans-2-hexenal ($C_6H_{10}O$)
121. Isovitexin ($C_{21}H_{20}O_{10}$)
122. β amyrin ($C_{30}H_{50}O$)
123. Taxifolin ($C_{15}H_{12}O_7$)
124. Arachidic acid ($C_{20}H_{40}O_2$)
125. Limonene ($C_{10}H_{16}$)
126. Geranial ($C_{10}H_{18}O$)
127. Apigenin ($C_{15}H_{10}O_5$)
128. Succinic acid ($C_4H_6O_4$)
129. Tridecylate ($C_{13}H_{26}O_2$)
130. Nonylate ($C_9H_{17}O_2$-)
131. Linoleic acid ($C_{18}H_{33}O_2$)
132. 2-phenylacetaldehyde (C_8H_8O)
133. Procyanidin B_2 ($C_{30}H_{26}O_{12}$)
134. Octacosanyl ferulate ($C_{38}H_{66}O_4$)
135. Methyl hexacosenoate ($C_{27}H_{52}O_2$)
136. 2-Furancarboxaldehyde ($C_5H_4O_2$)
137. 10-octadecenoic acid ($C_{18}H_{35}O_2$)
138. Hexadecanoic acid ($C_{19}H_{38}O_2$)

The I-TASSER generated target protein model was subjected to Ramachandran plot analysis and the result revealed that 75% of amino acid residues are present in most favoured region. Neutral PLA2 RVV-PFIIc exerts its strong anticoagulant effect and also causes intravascular haemolysis. [20] MetaPocket showed 7 amino acid residues, among them Val10, the non-polar hydrophobic residue was identified as active residue for docking. L-amino acid oxidase belongs to the enzyme class oxidoreductases that catalyze the stereospecific oxidative deamination of L-amino acids. Snake venom LAAOs are usually homodimeric with cofactors FAD (Flavin Adenine Dinucleotide) or FMN (Flavin Mononucleotide) covalently linked to their chemical structure. The yellow colour of venom rich in these enzymes is related to the presence of the pigment riboflavin present in the cofactors. During enzymatic reaction LAAO produce hydrogen peroxide and ammonia which induce cell membrane permeability, necrosis and apoptosis. LAAO exert biological and pharmacological effects, including actions on platelet aggregation and the induction of apoptosis, hemorrhage, and cytotoxicity. [21] The selected sequence of LAAO has 138 amino acids sequence and BLASTp analysis showed 89% identity, 100% query cover and an E-value of 4e-97 with native L-amino acid oxidase from Vipera ammodytes ammodytes A chain (PDB id-3KVE) and it was taken as the template for

modelling. Ramachandran plot analysis revealed 80% of the residues were in most favoured region. The MetaPocket generated ligand binding sites of LAAO contains 130 amino acid residues from that the residue His241 was selected as critical residue. Cytotoxin drCT-1 has anti-proliferative, cytotoxic and apoptotic activities. Also induce neurotoxicity, cardiotoxicity and myotoxicity. It consists of 20 amino acid sequence and the BLASTp results showed 100% identity, 100% query cover and an E-value of 9e-16 with cardiotoxin analogue V from the Taiwan cobra (*Naja naja atra*) (PDB id-1CHV) and it was taken as template for modelling.

Table 2: Docked results of hit molecules from *Phyllanthus emblica*

Target Protein	Hit Molecules	ΔG_{bind} (Kcal/mol)	Ki	H-Bond	H-Bond residues	Bond Length (Å)
Basic PLA2 VRV-PL-VIIIa	Stigmasterol	-11.34	4.87 nM	O-H-O	Ala18	3.21
	β-sitosterol	-11.11	7.18 nM	Nil		
	Campesterol	-10.94	9.57 nM	O-H-O	Ala18	3.18
	Lupenone	-9.86	58.91 nM	Nil		
	Betulonic acid	-9.75	71.31 nM	O-H-O	Arg43	2.62
Anticoagulant class II PLA2	β-sitosterol	-10.70	14.32 nM	Nil		
	Lupeol	-10.34	26.40 nM	Nil		
	Campesterol	-9.97	48.93 nM	O-H-O	Pro18	2.67
				O-H-O	Ser23	3.05
	Friedelan-3-one	-9.83	62.21 nM	Nil		
	Betulin	-9.19	184.92 nM	Nil		
	β-Amyrinketone	-10.88	10.66 nM	Nil		
Acidic PLA2 Drk-a1	Betulinic acid	-10.85	11.16 nM	O-H-O	Ala33	2.69
				N-H-O	Lys76	2.81
	β-sitosterol	-9.96	50.21 nM	O-H-O	Ala33	2.62
	Stigmasterol	-9.82	63.02 nM	O-H-O	Ala33	2.91
	Lupeol	-9.75	70.93 nM	Nil		
Neutral PLA2 RVV-PFIIc	Stigmasterol	-6.89	8.91 uM	O-H-O	Glu7	3.11
	Betulonicacid	-6.81	10.23 uM	Nil		
	Campesterol	-6.78	10.77 uM	O-H-O	Glu7	3.07
	β-Amyrinketone	-6.71	11.97 uM	Nil		
	Friedelan-3-one	-6.59	14.66 uM	Nil		
L-Aminoacid oxidase	Stigmasterol	-14.41	27.46 pM	O-H-O	Cys311	2.74
	β-sitosterol	-14.03	51.61 pM	O-H-O	Cys311	2.64
	Betulonic acid	-13.90	65.15 pM	Nil		
	Lupenone	-13.89	65.46 pM	N-H-O	Met61	3.07
	Betulin	-13.85	70.88 pM	N-H-O	Met61	2.81
				O-H-O	Tyr390	2.67
Russell's viper venom serine proteinase, RVV-V	Stigmasterol	-10.62	16.54 nM	O-H-O	Leu99	2.91
	β-sitosterol	-10.43	22.72 nM	O-H-O	Leu99	2.88
	Campesterol	-9.99	47.17 nM	O-H-O	Leu99	2. 57
	Quercetin	-6.88	9.11 uM	O-H-O	Ser217	3.18
				O-H-O	Thr190	2.70
				O-H-O	Thr190	2.84
				O-H-O	Ala214	3.09
	Catechin	-6.84	9.62 uM	N-H-O	Arg60	2.95
				O-H-O	Ser217	2.79
				O-H-O	Thr190	2.45
				O-H-O	Ser195	2.54
Cytotoxin drCT-1	Betulinicacid	-8.67	443.01 nM	O-H-O	Leu20	1.583
				O-H-O	Lys5	2.222
				O-H-O	Lys5	2.185
	Betulonicacid	-7.66	2.42 uM	N-H- O	Lys5	2.60
	Betulin	-7.30	4.48 uM	N-H-O	Leu20	2.47
				N-H-O	Asn4	2.57
Dabocetin alpha subunit	β-Amyrinketone	-7.12	6.02 uM	Nil		
	Friedelan-3-one	-7.00	7.39 uM	Nil		
	Betulonicacid	-7.03	6.99 uM	O-H-O	Thr116	2.76
	Friedelan-3-one	-6.79	10.62 uM	Nil		
	β-Amyrinketone	-6.62	14.08 uM	N-H-O	Lys86	2.63
	Stigmasterol	-6.55	15.72 uM	O-H-O	His133	2.96
				O-H-O	Glu50	3.05
	Betulin	-6.45	18.61 uM	O-H-O	Arg94	2.70
				N-H-O	Gln96	3.09
Cysteine-rich seceretory protein Dr-CRPK	Friedelan-3-one	-9.64	85.77 nM	Nil		
	Lupenone	-9.51	106.62 nM	N-H-O	Asn187	2.87
	β-Amyrinketone	-9.17	190.14 nM	Nil		
	Lupeol	-8.83	337.46 nM	Nil		
				N-H-O	Ile113	3.09
	Betulonicacid	-8.78	369.34 nM	N-H-O	Arg63	2.81
				N-H-O	Lys123	3.04

Table 3: Docked results of hit molecules from *Tamarindus indica*

Target Protein	Hit Molecules	$\Delta G_{bind\ (Kcal/mol)}$	Ki	H-Bond	H-Bond residues	Bond Length (Å)
Basic PLA2 VRV-PL-VIIIa	β amyrin	-12.74	2.66 nM	N-H-O, O-H-O	Gly30 Tyr28	3.00 2.77
	Lupanone	-11.37	4.63 nM	Nil		
	Stigmasterol	-11.34	4.87 nM	O-H-O	Ala18	3.21
	β-Sitosterol	-11.11	7.18 nM	Nil		
	Campesterol	-10.94	9.57 nM	O-H-O	Ala18	3.18
Anticoagulant class II PLA2	β amyrin	-10.96	9.29 nM	O-H-O	Tyr28	2.68
	β-Sitosterol	-10.70	14.32 nM	Nil		
	Lupeol	-10.34	26.40 nM	O-H-O	Cys45	2.47
	Lupanone	-10.05	42.68 nM	Nil		
	Campesterol	-9.97	48.93 nM	O-H-O O-H-O	Pro18 Ser23	2.77 2.71
Acidic PLA2 Drk-a1	Lupanone	-10.34	26.15 nM	Nil		
	β amyrin	-10.02	45.03 nM	O-H-O N-H-O	Gly45 Gly47	2.96 2.90
	β-Sitosterol	-9.96	50.21 nM	O-H-O	Ala33	2.62
	Stigmasterol	-9.82	63.02 nM	O-H-O	Ala33	2.91
Neutral PLA2 RVV-PFIIc	Lupeol	-9.75	70.93 nM	Nil		
	Stigmasterol	-6.89	8.91 uM	O-H-O	Glu7	3.11
	Campesterol	-6.78	10.77 uM	O-H-O	Glu7	2.97
	Lupanone	-6.60	14.45 uM	Nil		
	β amyrin	-6.16	30.40 uM	O-H-O N-H-O	Ala17 Ala17	2.61 3.15
	Lupeol	-6.12	32.58 uM	Nil		
L-Aminoacid oxidase	Stigmasterol	-14.41	27.46pM	O-H-O	Cys311	2.74
	β-Sitosterol	-14.03	51.61 pM	O-H-O	Cys311	2.64
	β amyrin	-13.25	192.95 pM	O-H-O	Arg108	3.02
	Lupanone	-12.86	376.22 pM	N-H-O	L ys344	2.88
	Cycloartanol	-12.77	436.23 pM	O-H-O O-H-O	Glu237 His481	2.74 2.99
Russell's viper venom serine proteinase, RVV-V	Stigmasterol	-10.62	16.54 nM	O-H-O	Leu99	2.91
	β-Sitosterol	-10.43	22.72 nM	O-H-O	Leu99	2.88
	Campesterol	-9.99	47.17 nM	O-H-O	Leu99	2.57
	Cycloartanol	-7.24	4.95 uM	O-H-O O-H-O O-H-O	Ala214 Asp102 Thr190	2.63 2.59 2.88
	Apigenin	-7.15	5.76 uM	O-H-O O-H-O N-H-O	His 57 His 41 Arg 60	2.84 2.65 3.25
Cytotoxin drCT-1	Lupanone	-7.66	2.42 uM	Nil		
	β amyrin	-7.59	2.74 uM	O-H-O S-H-O	Leu20 Cys14	2.43 2.85
	Cycloartanol	-6.81	10.12 uM	O-H-O	Leu20	2.79
	β-Sitosterol	-6.72	11.87 uM	O-H-O	Leu20	2.79
Dabocetin alpha subunit	Lupeol	-6.58	14.91 uM	Nil		
	β amyrin	-7.02	7.16 uM	O-H-O	Glu47	2.66
	Lupanone	-6.70	12.36 uM	Nil		
	Stigmasterol	-6.55	15.72 uM	O-H-O	His133	2.96
	Lupeol	-6.34	22.71 uM	O-H-O	Asn72	2.98
	Campesterol	-6.06	36.25 uM	O-H-O	His133	2.87
Cysteine-rich secretory protein Dr-CRPK	Lupanone	-9.49	110.86 nM	Nil		
	β amyrin	-9.10	212.91 nM	O-H-O O-H-O	Asp193 Thr190	2.81 3.11
	Lupeol	-8.83	337.46 nM	Nil		
	Stigmasterol	-8.64	465.91 nM	O-H-O	Gly151	2.92
	β-Sitosterol	-8.62	481.79 nM	O-H-O	Asn187	2.80

Lue 9, the non-polar hydrophobic amino acid residue was selected as critical residue from the MetaPocket generated 10 amino acid residues. Dabocetin is a C-type lectin-like protein. C-type lectins are nonenzymatic proteins which are found in many animals and bind to mono- and oligosaccharides in a Ca^{2+}-dependent manner. Snake venom C-type lectin-like proteins (SV-CTLPs) are similar in structure to common C-type lectins like proteins and have different pharmacological actions on thrombosis and hemostasis as exogenous modulators. [22] Many SV-CTLPs can affect platelet function by binding to various platelet membrane glycoprotein receptors. Unlike other SV-CTLPs, dabocetin inhibits ristocetin-induced platelet agglutination in a dose-dependent manner in platelet-rich plasma. [23] Dabocetin is basically heterodimeric protein with two closely-related subunits, α and β, generally held together by a single disulphide bond, and they form an integrated structure by swapping loops. These proteins bind with high affinity to specific blood coagulation factors. For the present study, α- sub unit of the protein was selected which consists of 20

amino acid sequence and the BLAST results showed 65% identity, 84% query cover and an E-value of 3e-57 with chain A of Bitiscetin, A Von Willeband Factor-Dependent Platelet Aggregation Inducer from Bitis arietans (puff adder) (PDB id-1JWI) and it was selected as template for modelling. Ramachandran plot analysis through PdbSum was carried out and result revealed that 90% of the residues were present in most favoured region. MetaPocket generated ligand binding site contains nine amino acid residues, from that the catalytic residue Asp28 was selected as active residue for docking. Cysteine-Rich Secretory Protein (CRISP) is widely distributed in snake venoms and that they inhibit smooth muscle contraction and cyclic nucleotide-gated ion channels. [24]

Cysteine-Rich Secretory Protein DrCRPK selected sequence consists of 239 amino acids and BLASTp results showed 80% identity, 92% query cover and an E-value of 4e-135 with chain A of a crisp family Ca-channel blocker derived from venom of Protobothrops flavoviridis (PDB: 1WVR) and it was selected as template for modelling. Ligand binding site of the target protein contain 53 amino acid residues generated via MetaPocket. Phe 189 was selected as critical residue since it is present in the functional region (N-terminal loop) of CRISP and act as interface between CRISP and other molecules because of its exposed conformation. [25-26]

Phyllanthus emblica

Analysis of the docked results between 79 phytochemicals obtained from *P. emblica* and each of the venom protein revealed that the plant contains potential inhibitory molecules against viper venom proteins. Out of 79 phytochemicals 49 showed ΔGbind ≤-5Kcal/mol against basic PLA2 VRV-PL-VIIIa. Top five molecules with least free energy of binding were further analysed based on H-bond and other interactive force fields and the compound stigmasterol was selected as the best lead since it has lowest binding energy (ΔGbind -11.34Kcal/mol) and established an H-bond with Ala18 of the target.

Against anticoagulant class II PLA2, 39 molecules showed inhibitory activity (ΔGbind≤-5Kcal/mol). Of these, β-sitosterol showed least free energy of binding (-10.70 kcal/mol), followed by lupeol (-10.34 Kcal/mol), friedelan-3-one (-9.83 Kcal/mol) and campesterol (-9.97 Kcal/mol) respectively. Except campesterol others did not show any hydrogen bond, but considering the significant difference in free energy level the compound β-sitosterol was selected as the best lead. Forty-nine phytochemicals showed ΔGbind≤-5 Kcal/mol against acidic PLA2 Drk-a1, of these, β amyrin ketone showed least free energy of binding (-10.88 Kcal/mol) followed by betulinic acid (-10.85 Kcal/mol). The binding energy between these two molecules with acidic PLA2 Drk-a1 was insignificant and the latter has established two hydrogen bonds with residues in the active site and therefore, betulinic acid was recommended as the best lead. Twenty two phytochemicals has inhibitory activity (ΔGbind≤-5Kcal/mol) on , neutral PLA2 RVV-PFIIc, of these stigmasterol showed least free energy of binding (-6.89 Kcal/mol) with a hydrogen bond at active site residue and selected as lead molecule. Against L-amino acid oxidase, 65 phytochemicals showed ΔGbind≤-5Kcal/mol and the compound stigmasterol and β-sitosterol showed least free energy of binding -14.41Kcal/mol and -14.03Kcal/mol respectively and each compound have established a hydrogen bond with active residue Cys311 of the target molecules. Both compounds are equally competent for recommending as the best lead but considering the negligible difference in free energy level the compound stigmasterol was suggested as the best lead. Similarly, a total 27 phytochemicals showed inhibitory activity on Russell's viper venom serine proteinase RVV-V and the compounds stigmasterol and β-sitosterol showed ΔGbind -10.62 and -10.43 Kcal/mol respectively. These compounds have hydrogen bond with residue Leu99 in the active site. Both compounds are equally qualified for selecting as lead molecule, however, considering the negligible difference in energy level stigmasterol was selected as the lead.

Table 4: Molsoft analysis of lead molecules

Hit molecules	Molecular formula	Molecular weight [g/mol]	HBA/ HBD	MolLogP	MolLogS (mg/L)	MolPSA A^2	Drug-likeness score
Apigenin	$C_{15}H_{15}NO_3$	257.11	3/1	1.93	210.05	43.86	0.53
Betulin	$C_{30}H_{50}O_2$	442.38	2/2	*7.90	0.04	33.21	-0.09
Betulinic acid	$C_{30}H_{48}O$	456.36	3/2	*7.65	0.06	44.50	0.31
Betulonic acid	$C_{30}H_{46}O_3$	454.34	3/1	*7.35	0.04	42.13	0.64
Campesterol	$C_{28}H_{48}O$	400.37	1/1	*8.90	0.02	16.28	0.71
Catechin	$C_{15}H_{14}O_6$	290.08	6/5	1.88	166.49	90.45	0.92
Cycloartanol	$C_{30}H_{52}O$	428.40	1/1	*9.49	0.01	16.43	-0.57
Friedelan-3-one	$C_{30}H_{50}O$	426.39	1/0	*8.81	0.00	13.36	-0.48
Lupanone	$C_{30}H_{50}O$	426.39	1/0	*9.02	0.00	13.73	0.38
Lupenone	$C_{30}H_{48}O$	424.37	1/0	*8.72	0.00	13.73	0.37
Lupeol	$C_{30}H_{50}O$	426.39	1/1	*9.02	0.00	16.09	-0.16
Quercetin	$C_{15}H_{10}O_7$	302.04	7/5	2.11	40.95	102.61	0.93
Stigmasterol	$C_{29}H_{48}O$	412.70	1/1	*8.82	0.01	16.28	0.73
β-Amyrin	$C_{30}H_{50}O$	426.39	1/1	*9.17	0.00	15.73	-0.23
β-Amyrinketone	$C_{30}H_{48}O$	424.37	1/0	*8.87	0.00	13.36	-0.02
β-sitosterol	$C_{29}H_{50}O$	414.70	1/1	*9.48	0.01	16.28	0.88

*indicates violation of Rule of Five

A total 39 phytochemicals qualified as hit molecules against cytotoxin drCT-1, of these betulinic acid showed least binding energy (-8.67 Kcal/mol) and three hydrogen bonds with residues in the active site and selected as lead molecule against the protein. Eighteen phytochemicals showed inhibitory effect (ΔGbind≤-5Kcal/mol) on dabocetin alpha subunit, among them betulonic acid has least free energy of binding (-7.03Kcal/mol) and a hydrogen bond and suggested as the lead. Against cysteine-rich secretory protein Dr-CRPK, 47 phytochemicals showed ΔGbind≤-5Kcal/mol and these molecules were considered as hit molecules. Of these, the compounds friedelan-3-one and lupenone showed least free energy of binding -9.64 Kcal/mol and -9.51 Kcal/mol respectively. The energy difference between these two compounds was insignificant and both compounds are equally competent as lead. However, the latter molecule has a hydrogen bond with Asn187 in the active site and therefore lupenone was selected as the lead. Details of hit molecules against each protein were depicted in Table 2.

Tamarindus indica

A total 59 phytochemicals were docked with each of the nine selected viper venom proteins and the results indicated that the plant contains many phytochemicals for inhibiting all the targets. Forty six phytochemicals showed (ΔGbind≤-5Kcal/mol) inhibitory activity on basic PLA2 VRV-PL-VIIIa, of these the compound β amyrin was selected as the lead molecule since it has least free energy of binding (-12.74Kcal/mol), inhibition constant (KI) and two hydrogen bonds. Similarly, against anticoagulant class II PLA2, 30 phyomolecules showed inhibitory activity and β amyrin has least free energy of binding (-10.97 Kcal/mol), KI and H-bond, and selected as lead molecule. Thirty two phytochemicals showed inhibitory effect on acidic PLA2 Drk-a1, among them lupanone showed least binding energy (-10.34 Kcal/mol) and KI. The compound β amyrin showed ΔGbind -10.02 Kcal/mol and two H-bonds with acidic PLA2 Drk-a1, however, its KI value was higher and binding energy level was also comparatively high and therefore lupanone was selected as the lead. Against neutral PLA2 RVV-PFIIc, 13 phytochemicals showed (ΔGbind≤-5Kcal/mol) inhibitory activity and stigmasterol was selected as the lead since it has least free energy of binding (-6.89 Kcal/mol), KI and one H-bond. Similarly out of 41 phytomolecules identified as inhibitors against L-amino acid oxidase, the compound stigmasterol showed least free energy of binding (-14.41Kcal/mol), KI and one H-bond and therefore selected as the lead. The same compound was identified as lead against Russell's viper venom serine proteinase RVV-V since it showed least free energy of binding, KI and an H-bond. Fifteen phytochemicals has inhibitory activity on cytotoxin drCT-1, of these the compound lupanone showed least binding energy (-7.66 Kcal/mol) and KI but no H-bond. The compound β amyrin showed negligible difference in binding energy (-7.59 Kcal/mol) and KI value and has two H-bonds. In this circumstance both compounds were suggested as the lead molecules. Against dabocetin alpha subunit, only nine phytochemicals showed inhibitory activity and β amyrin was selected as the lead since it has least free energy of binding (ΔGbind-7.02Kcal/mol), KI and an H-bond. A total 19 phytochemicals showed inhibitory activity on cysteine-rich secretory protein Dr-CRPK, of these lupanone showed least free energy of binding (-9.49Kcal/mol) and KI value and suggested as lead molecule. Here also β amyrin showed negligible difference in binding energy and two H-bonds but KI value was higher. Details of hit molecules against each protein were depicted in Table 3. Molecular and drug-likeness properties of hit molecules from each plant against all the target proteins were analysed using the tool Molsoft (Table 4). All the leads comply with the Rule of five properties except lipophilicity (MolLogP value) while apigenin, catechin and quercetin are the leads fully obeyed with the rules. A number of drugs derived from natural products are effectively been administering though they violate one or two of the five rules. Among the currently available drugs 16% of them are not fully agree with the Rule of five whereas free energy of binding and H-bond analysis got prima face importance. [27] Docked structure of all the selected lead molecules derived from both plants with targets was depicted on Fig. 2 & 3.

The overall results indicated that the compounds viz β-sitosterol, betulonicacid, campesterol, phyllaemblic acid, phyllantidin and stigmasterol isolated from the plants showed inhibitory activity on all the nine Russell's viper venom proteins. Nisha *et al.* [28] reported that the forgoing molecules derived from different plant species shown inhibitory effect on cobra venom multiple proteins. Several, plant derived molecules exhibited multiple target inhibitory activity and it is well acknowledged that such compounds are superior than single target oriented drug molecule when applied on complex system like human body with unpredictable physiological condition. [29] The results indicated that a standardized combination of these molecules can effectively inhibit the venom proteins of different snake species. Further in-depth analysis in this line will leads to the discovery of plant derived novel drugs against snakebite. The results revealed that both the plants *P. emblica* and *T. indica* contain potential lead molecules which can effectively inhibit/neutralize toxic viper venom proteins. Even though it substantiate the traditional knowledge and previous *in vitro* and *in vivo* results, further investigation on a biological system is necessary for developing promising drug molecules.

ACKNOWLEDGEMENT

We thank SC/ST Department, Government of Kerala for financial support, Dr. T. Madhan Mohan, Senior

advisor (Retd.), Department of Biotechnology, Govt. of India and Director, JNTBGRI for providing the facilities and encouragements.

REFERENCES

1. http://www. who.int/neglected_diseases/ diseases/en/ accessed on 03/10/2017.
2. Mohapatra B, Warrell DA, Suraweera W, Bhatia P, Dhingra N, Jotkar RM, Rodriguez PS, Mishra K, Whitaker R, Jha P. Million Death Study Collaborators. Snakebite mortality in India: A nationally representative mortality survey. PLoS Neglected Tropical Diseases. 2011; 5(4):e1018.
3. Antonypillai CN, Wass JA, Warrell DA, Rajaratnam HN. Hypopituitarism following envenoming by Russell's vipers (*Daboia siamensis* and *D. russelii*) resembling Sheehan's syndrome: First case report from Sri Lanka, a review of the literature and recommendations for endocrine management. QJM: An International Journal of Medicine. 2010; 104:97-108.
4. Warrell DA. Clinical toxicology of Snake bites in Asia. In: White MA, ed. Handbook of clinical toxicology of animal venoms and poisons. CRC Press, 1995.
5. Warrell DA. Snake venoms in science and clinical medicine. 1. Russell's viper: Biology, venom and treatment of bites. Trans R Soc Trop Med Hyg. 1989; 83:732-740.
6. Nisha NC, Sreekumar S, Biju CK, Krishnan PN. Snake antivenom: Virtual screening of plant-derived molecules. Biobytes. 2010; 6:14-22.
7. Kang TS, Georgieva D, Genov N, Murakami MT, Sinha M, Kumar RP, Kaur P, Kumar S, Dey S, Sharma S, Vrielink A. Enzymatic toxins from snake venom: Structural characterization and mechanism of catalysis. FEBS J. 2011; 278(23):4544-4576.
8. Nisha NC, Sreekumar S, Biju CK, Krishnan PN. Identification of lead compounds with cobra venom neutralising activity in three Indian medicinal plants. Int J Pharm Pharm Sci. 2014; 6: 536-541.
9. Alam MI, Gomes A. Snake venom neutralization by Indian medicinal plants (*Vitex negundo* and *Emblica officinalis*) root extracts. J Ethnopharmacol. 2003; 86:75-80.
10. Ushanandini S, Nagaraju S, Harish Kumar K, Vedavathi M, Machiah DK, Kemparaju K, Vishwanath BS, Gowda TV, Girish KS. The anti-snake venom properties of *Tamarindus indica* Leguminosae) seed extract. Phytother. Res. 2006; 20:851-858.
11. Arnold K, Bordoli L, Kopp J, Schwede T. The SWISS-MODEL Workspace: A web-based environment for protein structure homology modelling. Bioinformatics. 2006; 22:195-201.
12. Ramachandran GN, Sasisekharan V. Conformation of polypeptides and proteins. Vol. 23, Adv Protein Chem.1968, pp.283-438.
13. Roy A, Kucukural A, Zhang Y. I-TASSER: A unified platform for automated protein structure and function prediction. Nature Protocols. 2010; 5(4):725-738.
14. Deepa V, Sreekumar S, Biju CK. Validation of Russell's Viper Venom Detoxification Activity of *Azadirachta indica* through *In silico* Method. IOSR J Pharm Biol Sci. 2016; 11:35-46.
15. Warrell DA. Snake venoms in science and clinical medicine. Russell's viper: Biology, venom and treatment of bites. Trans. R. Soc. Trop. Med. Hyg. 1989; 83(6):732-740.
16. WHO. Guidelines for the management of snakebites. New Delhi, India, 2016.
17. Kang TS, Georgieva D, Genov N, Murakami MT, Sinha M, Kumar RP, Kaur P, Kumar S, Dey S, Sharma S, Vrielink A. Enzymatic toxins from snake venom: Structural characterization and mechanism of catalysis. FEBS J. 2011; 278(23):4544-4576.
18. Fatima L, Fatah C. Pathophysiological and Pharmacological Effects of Snake Venom Components: Molecular Targets. J Clin Toxicol. 2014; 4(190):2161-0495.
19. Jayanthi GP, Gowda TV. Geographical variation in India in the composition and lethal potency of Russell's Viper (*Vipera russelli*) venom. Toxicon. 1988; 26(3):257-64.
20. Saikia D, Majumdar S, Mukherjee AK. Mechanism of *in vivo* anticoagulant and haemolytic activity by a neutral phospholipase A2 purified from *Daboia russelii* venom: Correlation with clinical manifestations in Russell's Viper envenomed patients. Toxicon. 2013; 76:291-300.
21. Izidoro LF, Sobrinho JC, Mendes MM, Costa TR, Grabner AN, Rodrigues VM, da Silva SL, Zanchi FB, Zuliani JP, Fernandes CFC, Calderon LA, Stábeli RG, Soares AM. Snake Venom L-Amino Acid Oxidases: Trends in Pharmacology and Biochemistry, Biomed Res Int. 2014; 2014:196-754.
22. Ogawa T, Chijiwa T, Oda-Ueda N, Ohno M. Molecular diversity and accelerated evolution of C-type lectin-like proteins from snake venom. Toxicon. 2005; 45(1):1-14.
23. Zhong SR, Jin Y, Wu JB, Chen RQ, Jia YH, Wang WY, Xiong YL, Zhang Y. Characterization and molecular cloning of dabocetin, a potent antiplatelet C-type lectin-like protein from *Daboia russellii siamensis* venom. Toxicon. 2006; 47(1):104-112.
24. Yamazaki Y, Morita T. Structure and function of snake venom cysteine-rich secretory proteins. Toxicon. 2004; 44(3):227-31.
25. Wang J, Shen B, Guo M, Lou X, Duan Y, Cheng XP, Teng M, Niu L, Liu Q, Huang Q, Hao Q. Blocking effect and crystal structure of natrin toxin, a cysteine-rich secretory protein from *Naja atra* venom that targets the BKCa channel. Biochemistry. 2005; 44(30):10145-52.
26. Guo M, Teng M, Niu L, Liu Q, Huang Q, Hao Q. Crystal structure of the cysteine-rich secretory protein stecrisp reveals that the cysteine-rich domain has a K+ channel inhibitor-like fold. J. Biol. Chem. 2005; 280(13):12405-12412.
27. Bickerton GR, Paolini GV, Besnard J, Muresan S, Hopkins AL. Quantifying the chemical beauty of drugs. Nature Chemistry. 2012; 4(2):90.
28. Nisha NC, Sreekumar S, Biju CK. Identification of lead compounds with cobra venom detoxification activity in *Andrographis paniculata* (burm. F.) Nees through *in silico* method. Int J Pharma Pharm Sci. 2016; 8: 7:212-217.
29. Lu J-J, Pan W, Hu YJ, Wang YT. Multi-Target Drugs: The Trend of Drug Research and Development. PLoS ONE. 2012; 7:6:e40262.

HOW TO CITE THIS ARTICLE: Deepa V, Sreekumar S, Biju CK. *In silico* Validation of Anti-Russell's Viper Venom Activity in *Phyllanthus emblica* L. and *Tamarindus indica* L. Int. J. Pharm. Sci. Drug Res. 2018; 10(4): 217-226. **DOI: 10.25004/IJPSDR.2018.100403**